Radiotherapy and Oncology 141 (2019) 312–320

Contents lists available at ScienceDirect

Radiotherapy and Oncology

journal homepage: www.thegreenjournal.com

Original Article

Estimation of inter-fractional variations in interstitial multi-catheter breast brachytherapy using a hybrid treatment delivery system

Karoline Kallis, Nadin Abu-Hossin, Stephan Kreppner, Michael Lotter, Vratislav Strnad, Rainer Fietkau, Christoph Bert *

Department of Radiation Oncology, Universitätsklinikum Erlangen, Friedrich-Alexander-Universität Erlangen-Nürnberg (FAU), Erlangen, Germany

ARTICLE INFO

Article history:
Received 22 May 2019
Received in revised form 13 August 2019
Accepted 14 August 2019
Available online 5 September 2019

Keywords:
Breast cancer
Interstitial multi-catheter brachytherapy
Electromagnetic tracking
Inter-fractional variations

ABSTRACT

Purpose: Irradiation of the tumor bed using interstitial multi-catheter brachytherapy is one of the treatment options for breast cancer patients. In order to ensure the planned dose delivery an advanced quality intervention method using an electromagnetic tracking (EMT) system is presented. The system is used to assess inter-fractional variations within the framework of a patient study.
Methods and materials: Until now 41 patients were included in the study for the evaluation and overall 355 EMT measurements were performed. The catheter traces are measured automatically and sequentially using an afterloader prototype (Flexitron, Elekta, Veenendaal, The Netherlands) equipped with an EMT sensor. The implant geometry is tracked directly after implantation, after CT imaging and after each irradiation fraction. The acquired data is rigidly registered to the catheter traces defined in the treatment plan and the dwell positions (DP) are reconstructed. DPs defined in treatment planning serve as reference. Breathing motion was corrected and recorded using three reference 6DoF sensors placed on the patients' skin. The Euclidean distance between the planned and reconstructed DPs provides information about possible inter-fractional deviations. Further, the influence of various factors on the occurrence of large deviations was investigated, like the patients' age, the length of the catheter, the breast volume, etc.
Results: Over all patient measurements a median Euclidean distance of 2.19 mm was determined between the reconstructed DPs and the reference DPs. The median deviation combining all datasets was minimal (1.67 mm) at the measurement directly after CT imaging. The deviations between the different fractions have a median distance of 2.31 mm which could be improved to 2.05 mm by adapting the treatment plan according to the follow-up CT. No correlation between the distance to the skin, ribs, mammilla or the breast volume and the occurrences of large deviations was found. The largest deviations were determined in the upper inner quadrant of the breast.
Conclusion: The afterloader prototype could be well integrated into the clinical routine and is beneficial for ensuring the quality of the brachytherapy. Overall, a small median DP deviation, lower than the used step size of 2.5 mm, was detected.
 Radiotherapy and Oncology 141 (2019) 312–320

Accelerated partial breast irradiation (APBI), using high-dose rate (HDR) interstitial multi-catheter brachytherapy (iBT), is a treatment option after breast conserving surgery and proved to be non-inferior to whole breast irradiation for a selected patient population considering local recurrence rate, disease free survival, overall survival, quality of life, late side effects and cosmetic outcome [1–7].

For optimal quality assurance particularly regarding the planned dose delivery, it is important to minimize the occurrence of clinical uncertainties, given that due to steep dose gradients small deviations could have a considerable impact on the dose delivery [8,9].

Various studies investigated the benefit of *in-vivo* dosimetry for real-time treatment verification and source tracking in brachytherapy [10–12]. Moreover, using a flat panel detector for imaging and source tracking proved to be beneficial and showed that on average the planned dwell positions (DP) differ up to 0.60 mm to the measured DP [13]. Beaulieau et al. [14] introduced a real-time treatment platform for prostate HDR brachytherapy, combining electromagnetic tracking (EMT) and 3D ultrasound imaging (TRUS) to improve treatment quality. Bert et al. [15] demonstrated the potential of EMT for error detection mainly prior to irradiation, like the malfunction of the afterloader, the verification of the patient

* Corresponding author at: Strahlenklinik, Universitätsklinikum Erlangen, Universitätsstraße 27, 91054 Erlangen, Germany.
E-mail addresses: karoline.kallis@fau.de (K. Kallis), christoph.bert@uk-erlangen.de (C. Bert).

https://doi.org/10.1016/j.radonc.2019.08.012
0167-8140/

specific implant, intra- and inter-fractional applicator movements and interchanged transfer tubes. Damato et al. [16] investigated the use of EMT for quality assurance in brachytherapy using phantoms. Kellermeier et al. [17,18] summarized the advantages of EMT systems for quality assurance in iBT for breast cancer patients and showed first results of the assessment of inter-fractional changes.

In former publications we introduced a new hybrid afterloader prototype and suitable algorithms for advanced quality assurance in iBT and showed first patient and phantom results [19]. This manuscript peruses the previously introduced patient study, summarizes the results and observations estimated with the prototype in order to analyze inter-fractional changes.

Materials and methods

Patient cohort. Until now 41 female patients treated with multi-catheter HDR iBT were recruited between September 2016 and April 2019 for the study using the hybrid afterloader (see Table 1 for details). The study was approved by the institutional ethical committee of Friedrich-Alexander-Universität Erlangen-Nürnberg (NDI-HDR-1 355-14B, 2014) and all participants signed an informed consent. 30 of the 41 considered patients were treated with APBI and 11 patients only received an additional brachytherapy boost treatment. APBI patients usually received 9 fractions of 3.8 Gy and boost patients were irradiated with 2 fractions of 6 Gy, details see Supplementary materials and Figure 1a.

In total 699 catheters of 41 patients were analyzed. Additionally, these results were compared to a second patient cohort consisting of 28 patients treated in the period of January 2015 to May 2016. At that time, the catheter traces were manually measured with an EMT system by retracting a 5 degree of freedom (DoF) sensor. All details about the patient cohort and the study concept are summarized in Kellermeier et al. [18].

Treatment protocol. Image-guided treatment planning was performed according to the GEC-ESTRO guidelines [20–22], see section Supplementary materials for a precise description of the treatment protocol. For additional quality assurance a follow-up computed tomography (CT) with the same settings as the planning CT was acquired prior to the fifth fraction. The catheter traces were adapted according to the follow-up CT and keeping the DPs and DTs constant possible changes within the treatment plan were estimated.

EMT study protocol. The hybrid treatment delivery system described by Kallis et al. [19] was used for the EMT measurements.

Table 1
Patient specifications.
HDR = high-dose-rate; PTV = planning target volume; APBI = accelerated partial breast irradiation, DP = dwell position.

Parameter	Specification	Value
Number of patients	Total	41
	APBI	30
	Follow-up CT	23
	Boost	11
	Left breast	27
	Right breast	14
Age	Range	37–83 years
	Median	59 years
Recruitment Time		09/09/2016–05/04/2019
Number of Catheters	Range	11–23
	Mean	17
	Total	699
PTV	Range	18.07–215.83 ccm
	Mean	73.44 ccm
Breast volume	Range	125.25–1373.46 ccm
	Mean	591.13 ccm
Number of active DP	Range	77–399
	Mean	213

The arrangement consists of an afterloader prototype (Flexitron Elekta, Veenendaal, The Netherlands) with an EMT 5DoF sensor integrated into the check cable, combined with an EMT system (Aurora, NDI, Waterloo, Canada). The system automatically measures the catheter traces during an extra check cable run. The EMT measurements were integrated into the clinical treatment workflow after implantation (EMT_{bed}), after CT imaging ($EMT_{CT(1)}$) and after each nth fraction (EMT_{Fn}), see Figure 1a. The data were acquired for study purposes only and the possible changes within the treatment course were established although the therapy was never adapted. Nonetheless, swaps of catheters happened coincidently while connecting the prototype afterloader and thus do not mirror the treatment with the clinical afterloader correctly.

The EMT measurement was performed immediately after irradiation and the patients were asked to remain still until the measurement was finished successfully. Further, visible catheter shifts were not corrected prior to the measurement. Motion, e.g. breathing or speaking, was monitored with help of the reference 6DoF sensors fixed on the patient's breast.

Data evaluation. The data processing was performed using in-house developed algorithms [19]. Determined EMT-based catheter traces and reconstructed DPs were compared to those defined in treatment planning which serve as ground truth, see section Supplementary materials for a detailed description of the performed registration of the EMT traces to the CT defined traces and of the performed motion correction. The DPs were defined by the absolute distance between the connector end of the applicator and the actual DP along the catheter.

The occurrence of errors like catheter connection swaps and shifts and the reliability of the performed registration were verified visually. A measurement was counted as shifted when at least in one of the catheters a shift was visible. The Euclidian distance (ε) between the corresponding DPs from EMT measurement and treatment plan was calculated to detect possible errors and to predict inter-fractional changes.

In order to verify the determined deviations for 23 patients with follow-up CT and correct $EMT_{CT(2)}$ measurement, the catheter traces defined in treatment planning are compared to the adapted catheter traces based on the follow-up CT. The estimated deviations are then compared to the calculated deviations between the DP defined in treatment planning and the reconstructed DPs based on the $EMT_{CT(2)}$ measurement.

Also, the changes in the major directions (ε_{e1}, ε_{e2}, ε_{e3}) were separately analyzed using the principle component analysis (PCA), where ε_{e1} usually defines the catheter implantation direction. A median total registration error (TRE) between the measured catheter traces and reconstructed catheters in the TPS was determined. In contrast to ε the TRE considers all catheters and the total length of each catheter trace and thus quantifies the quality of the registration.

Further, the discrete Fréchet distance (δ_F) [23] was calculated between the catheter traces defined in the treatment plan and the measurement points. Both representations were smoothed by fitting a third degree polynomial through the data and both were sampled according to the measured absolute distances of the EMT measurement points. δ_F estimates the similarity of the reference data to the EMT measurement. In order to evaluate the quality of the measurement, the δ_F of the motion corrected smoothed data was compared to $\delta_{F\text{-}Raw}$ of the raw EMT data of the integrated 5DoF sensor. The resulting deviation ($\Delta\delta_F$) assesses distortion and motion of the EMT raw data in comparison to the corrected and smoothed EMT data.

For all reconstructed DPs and the reference DPs the convex hull volume (V) around all active DPs was assessed to obtain information about possible changes like swelling or shifts of catheters. To evaluate the implant volume changes (ΔV), the reference vol-

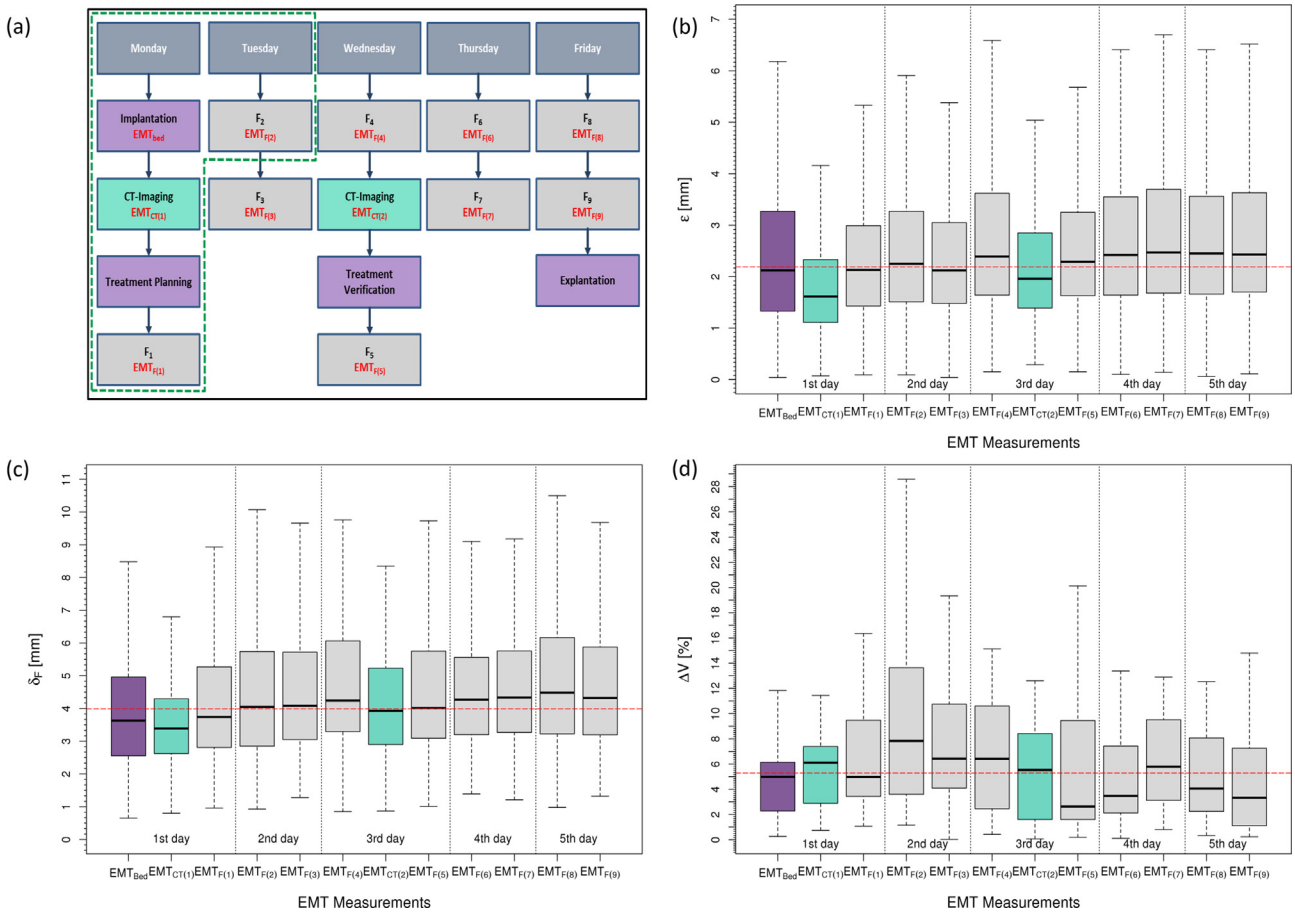

Figure 1. Evaluation of changes over the treatment course.
Subfigure (a) presents the overview of the typical treatment and measurement scheme. The dashed line in subfigure (a) marks the process for boost patients. For each measurement ε (subfigure (b)), δ_F (subfigure (c)) and ΔV (subfigure (d)) are presented. EMT_{bed} stands for the measurement directly after the implantation, $EMT_{CT(1)}$ shows the estimation of the measurement after CT imaging and EMT_{Fn} presents the deviations of each fraction, where n is the number of fractions. The dashed line shows the overall median value of the measurements. Outliers are not presented in the subfigure b, c and d.

ume (V_{CT}) and the estimated volumes, based on the reconstructed DPs of each EMT measurements (V_{EMT}), were compared.

The distance between the DPs and the skin and ribs OARs was determined by calculating for each DPs the Euclidian distance to the nearest point in the contour. The changes of the calculated distances (Δd_{ribs}, Δd_{skin}) relative to $EMT_{CT(1)}$ are reported.

Further, the correlation (ρ) between different variables (number of catheters, breast volume, PTV, distance to skin and ribs, catheter length, ΔV, motion amplitude) and ε was evaluated using the Spearman-rank correlation with a confidence level of 0.95.

The median error over the course of treatment (median patient deviation, MPD) was used for the correlation evaluation of the breast volume, the PTV, the number of DPs, the number of catheters and the age. For all other estimations the correlation analysis was performed for each measurement (mean measurement deviation, MMD). The length of each catheter was correlated to the mean catheter deviation estimated at each measurement.

Furthermore, centered at the mammilla and projected into the coronal plane the breast was divided into four different quadrants similar to Zhen et al. [24], in order to analyze the correlation of DP locations and the occurring deviations (ε). Moreover, the influence of the distance to the mammilla on the magnitude of ε was estimated.

Results

Corrupted or distorted catheter measurements, e.g. because of motion of the field generator (FG) during the measurement, swapped catheters, falsely stored data or omitted catheter traces, were excluded. In total 355 out of 398 measurements were used for the assessment of geometry changes. 11% of the measurements needed to be excluded because of technical problems ($N = 12|28\%$), physical discomfort ($N = 8|19\%$) of the patient or logistical problems with the clinical workflow ($N = 23|53\%$).

Additionally, out of 6072 catheter measurements 0.4% of the measured catheter traces could not be used and were excluded of the evaluation, because they were distorted or incorrect. By mistake swapped catheters occurred in a total of four measurements. In 10% of all measured catheter traces, shifts could be visually detected. By analyzing these classified and shifted catheters in detail, a mean shift magnitude of 4.18 ± 0.30 mm (range 0.22 mm–32.11 mm) was determined. Figure 2 presents the measured data and the calculated results of patient P015 (MPD = 1.53 mm). MMD of 1.08 mm, 3.15 mm, 2.37 mm and 2.00 mm were calculated for $EMT_{CT(1)}$, EMT_{F2}, EMT_{F3} and EMT_{F4}, respectively. At EMT_{F2} measurement two catheters were accidentally swapped which could be visually detected, see Figure 2d. At EMT_{F3} a shift (approximately 5.00 mm) in catheter seven was observed. Supplementary Figure 1 shows the result for patient P037 (MPD = 1.95 mm) with an enlarged standard deviation of 1.63 mm over the week of treatment. Supplementary Figure 2 presents the results of a typical patient P020 (MPD = 1.67 mm). A summary of the detailed patient information and determined result is presented in Supplementary Table 1.

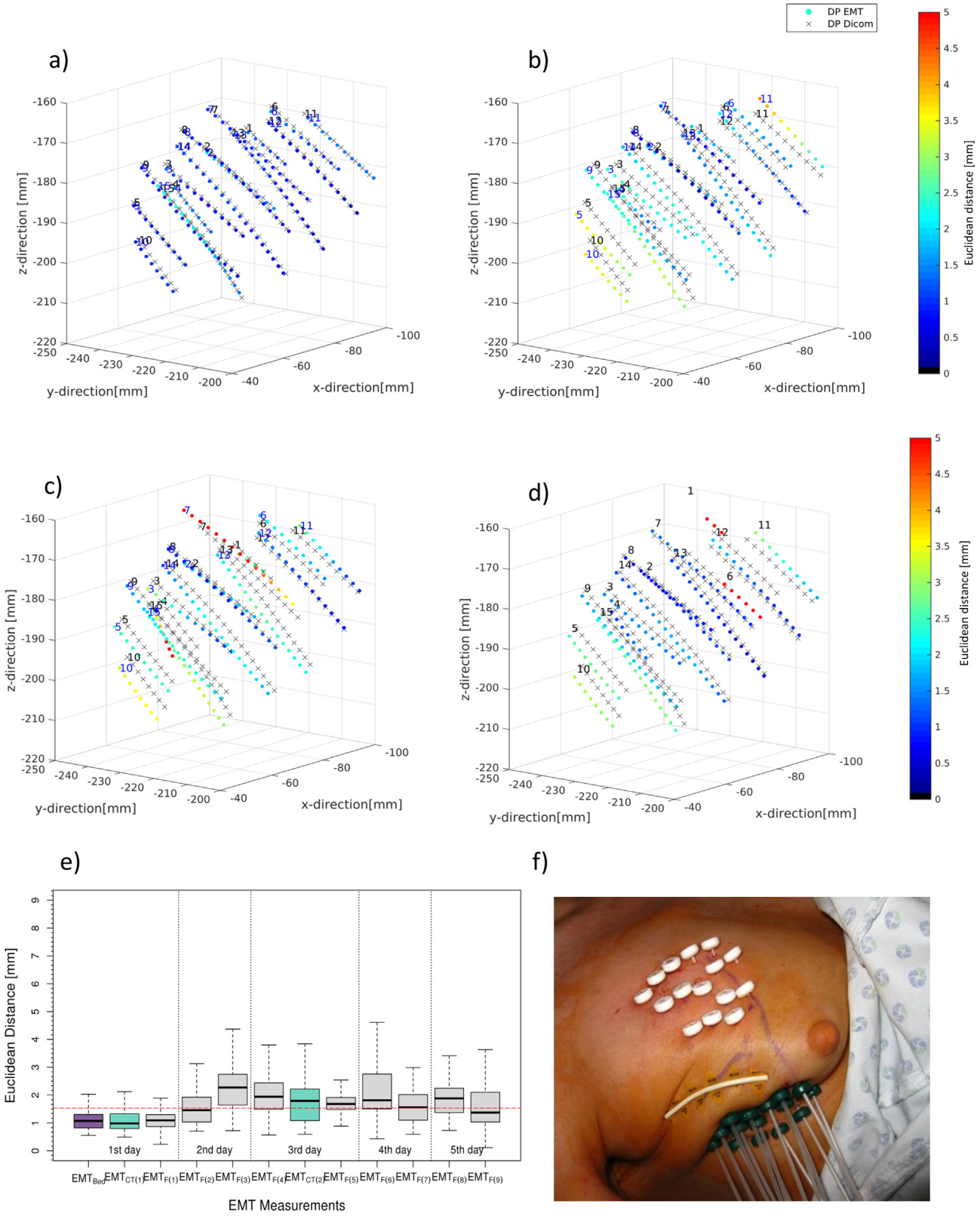

Figure 2. Overview of patient measurements.
The comparison of four different EMT measurements to the DPs defined in the treatment plan is presented. Subfigure a) shows the measurement directly after CT imaging. Subfigure b) the measurement after the fourth fraction. Subfigure c) shows the measurement after the third fraction with the 7th catheter shifted. Subfigure d) presents the measurement after the second fraction, where two catheters were accidently swapped. In order to indicate the magnitude of the deviations the Euclidian distance as color scale is defined. The crosses show the DPs defined in treatment planning. Subfigure e) shows the deviation over the course of treatment. The red dashed lines marks the overall median error determined for this patient. Subfigure f) presents the patient's breast with the implanted catheters directly after surgery.

Over all measurements a TRE of 1.58 ± 0.67 mm between the measured catheter traces and reconstructed catheters in the TPS was determined. All 69 patient datasets and all conducted measurements resulted in a median ε of 2.09 mm. The corresponding ε of the automatic measurement yielded a median value of 2.19 mm (mean 2.66 ± 1.98 mm, range 0.04 mm–19.74 mm) in comparison to 1.98 mm (mean 2.31 ± 1.54 mm, range 0.02 mm–11.52 mm) for the 28 patients with manual measurements. The MPD of the automatic measured patient cohort ranged between 1.46 mm and 4.08 mm.

All further detailed evaluations were performed with respect to the 41 patients for whom the implant geometry was automatically measured. All automatic patient measurements over the week of treatment resulted in a minimum median ε of 1.62 mm for $EMT_{CT(1)}$ and a maximum median ε of 2.47 mm for EMT_{F7}. However, the median of $EMT_{F1} - EMT_{F9}$ was determined to 2.31 mm. The overview of the ε changes on the different days is presented in Figure 1b. For the 23 APBI patients with available follow-up CT after the fourth fraction a median ε of 2.14 mm was calculated. The ε could be improved to 1.96 mm when using the adapted catheter traces based on the follow-up CT as reference after the 7th measurement ($EMT_{CT(2)}$). The maximal median ε after the 7th fraction of 2.47 mm was thus reduced to 2.00 mm.

The deviation between corresponding DPs determined between the treatment plan and the measurement ($EMT_{CT(2)}$) of the 23 APBI patients were on average 2.61 ± 1.96 mm. In contrast a mean deviation of 2.39 ± 1.82 mm was estimated between the DPs defined in treatment planning and the adapted DPs based on the follow-up CT, see also Supplementary Figure 3.

A mean Fréchet distance of 4.83 ± 3.95 mm was determined considering all automatic measurements. A weak correlation of the δ_F ($\rho = 0.63$) and ε was identified. $\delta_{F\text{-}Raw}$ was on average 8.81 ± 8.90 mm. On average $\Delta\delta_F$ was calculated to 4.84 ± 8.86 mm. Over all patients δ_F reached a minimum median value ($\delta_F = 3.39 \pm 1.25$ mm) at $EMT_{CT(1)}$ and a maximum median ($\delta_F = 4.48 \pm 2.15$ mm) at EMT_{F8}, details are shown in Figure 1c. No influence of the implantation direction on an enlarged δ_F could be proven, see Supplementary Figure 4 and Supplementary Figure 5.

Over all 41 patients a median ΔV of the volume encompassing all active DPs was determined to 5.28% (range 0.02%–57.62%). Throughout the treatment course, considering all patient measurements, the ΔV reached a maximum median at the second fraction of 7.83% and minimum median at the fifth fraction of 2.63%, see Figure 1d. Details of the results are summarized in Table 2.

For patients treated with an additional brachytherapy boost a larger ΔV, $\Delta\delta_F$, Δd_{ribs} and Δd_{skin} of 8.62 ± 9.68%, 6.50 ± 11.26 mm, 11.50 ± 15.47 mm and 6.40 ± 8.93 mm, respectively was proven in comparison to patients, which received an APBI treatment, see Table 2. Using the t-test (confidence level = 0.99) the differences between these groups proved to be significant ($p < 0.01$).

No correlation between the ε and breast volume ($\rho = 0.37$), PTV ($\rho = 0.39$), number of DPs ($\rho = 0.32$), number of implanted catheters ($\rho = 0.42$), patients' age ($\rho = 0.24$), distance to skin ($\rho = 0.32$), distance to ribs ($\rho = 0.38$), length of the catheters ($\rho = 0.09$), and ΔV ($\rho = 0.15$) could be found. Further, no correlation between the motion amplitude ($\rho = 0.18$) and ε and only a weak correlation between the migration in the principle components ($\rho(\varepsilon_1) = 0.65$; $\rho(\varepsilon_2) = 0.52$; $\rho(\varepsilon_3) = 0.53$) and the ε could be proven, thus the migration in implantation direction showed the greatest influence. However, ε is correlated to the TRE ($\rho = 0.82$), see Figure 3 for details. A dependence of ε and the distance to the surface or the ribs could not be proven. Nonetheless, we found first evidence that the patient's arm position has an impact on ε.

In the right/left breast 50%/52% of all DPs were located in the first upper inner, 27%/23% in the upper outer, 0.01%/18% in the lower outer and 23%/7% in the lower inner quadrant. A mean ε over all fractions of the right/left breast and all patients of 3.22 ± 2.60 mm/2.75 ± 1.97 mm, 2.68 ± 2.31 mm/2.49 ± 1.58 mm, 1.44 ± 0.59 mm/2.51 ± 1.56 mm and 2.87 ± 2.24 mm/2.61 ± 1.78 mm for upper inner, upper outer, lower outer and lower inner was estimated, respectively.

For both breast sides the upper inner quadrant shows overall the largest deviations. However, the deviations considering the right breast (2.99 ± 2.46 mm) were overall higher than the deviations on the left side (2.61 ± 1.79 mm). These findings are summarized in Figure 4 and in Supplementary Figure 6.

No correlation of the radius around the mammilla of each DP and an increase in ε could be proven ($\rho = 0.17$).

Discussion

The results show that the hybrid treatment delivery systems could be generally well integrated into the clinical workflow. However, in 23 of 398 EMT measurements the additional time incorporated prevented the performance of the EMT measurement. This drawback will be overcome when the EMT measurement and the irradiation are performed with the same afterloader and thus the most time consuming part, reconnecting the afterloader and the implanted catheters, can be eliminated. This is supported by a high acceptance of the patients as up to now no patient complained about discomfort during the measurement. Depending on the amount of implanted catheters the measurement takes 6–10 minutes and after importing the measurement data the computational time for analysis is approximately 10 s [19]. Given these findings, an online evaluation of existing deviations for quality assurance purposes prior to the irradiation should be possible.

Further, the system proved to be beneficial for detection of treatment errors and minimization of uncertainties in iBT, in order to improve the probability of a planned dose delivery. The current methodology for error detection is based on qualitative subjective visual validation. Quantitative analyses in phantom studies for error simulation and precise evaluations of the smallest possible detectable magnitude of shifts are ongoing [25].

The large deviation in the upper inner quadrant of the breast is connected to the most distal part of the catheters as well as in accordance with the mean implant direction. However, no explicit explanation, like the proximity to the axilla muscle, the for this effect could be proven and further patient data and measurements are needed for a reliable explanation.

The difference in ΔV, $\Delta\delta_F$, Δd_{ribs} and Δd_{skin} between the considered APBI and boost patients cohort are to this point not reasonable justifiable and seem to be caused by the individual patients rather than explicit characteristics of patients receiving an APBI treatment. More data of boost patients would be needed to prove this occurring effect.

One disadvantage of this study is that the irradiation source and the sensor are driven by decoupled drives, such that all DPs and applied DTs have to be simulated under the assumption that both drives and cables behave the same way. Hence, no verification of the actual applied dosage could be yielded [15]. However, using this hybrid system the occurrence of uncertainties might be quantified and decreased despite not gaining further insights of the exposed dose.

Considering all measurements, a minimal median ε of 0.98 mm was estimated for one patient's $EMT_{CT(1)}$ measurement. The minimal deviation is limited and influenced by various different causes, like the precision of the EMT sensor (0.70 mm), the registration (mean TRE 1.77 ± 0.66 mm), the positioning accuracy, which is dependent on the step motor, and the CT resolution (slice thickness = 2 mm) which has an influence on the user dependent precision of the catheter reconstruction (mean observer variability

Table 2
Summary of estimated deviations based on automatic EMT measurements.
ε = Euclidian distance between corresponding DPs; $\tilde{x}$ = median of variable x; IQR = interquartile range; $\bar{x}$ = mean of variable x; σ = standard deviation; min(x) = minimum of variable x; max(x) = maximum of variable x; ΔV = relative volume change; Δd_{ribs} = absolute distance change to the defined rib contour; Δd_{skin} = absolute distance change to the defined skin contour; ε_{ei} = error in direction; δ_F = Fréchet distance of catheters defined in treatment planning and measured catheter traces; $\Delta\delta_F$ = difference between Fréchet distance calculated with smoothed and raw measurement data.

Parameter		APBI	Boost	Total
ε [mm]	$\tilde{x}$	2.22	1.98	2.19
	IQR	1.77	1.48	1.75
	$\bar{x} \pm \sigma$	2.74 ± 2.02	2.31 ± 1.58	2.66 ± 1.98
	min(x)	0.04	0.04	0.04
	max(x)	19.74	13.52	19.74
TRE [mm]	$\tilde{x}$	1.58	1.46	1.58
	IQR	0.68	0.69	0.67
	$\bar{x} \pm \sigma$	1.77 ± 0.63	1.75 ± 0.90	1.77 ± 0.66
δ_F [mm]	$\tilde{x}$	4.05	3.60	3.99
	IQR	2.58	1.98	2.53
	$\bar{x} \pm \sigma$	4.87 ± 3.84	4.55 ± 4.89	4.83 ± 3.95
	min(x)	0.65	0.80	0.65
	max(x)	69.51	59.17	69.51
$\Delta\delta_F$ [mm]	$\bar{x} \pm \sigma$	4.67 ± 8.55	6.50 ± 11.26	4.84 ± 8.86
ΔV [%]	$\bar{x} \pm \sigma$	5.15 ± 7.40	8.62 ± 9.68	6.78 ± 6.59
Δd_{ribs} [mm]	$\bar{x} \pm \sigma$	5.82 ± 13.99	11.50 ± 15.47	6.25 ± 14.19
	$\tilde{x}$	1.08	2.08	1.12
	IQR	1.81	19.68	1.96
Δd_{skin} [mm]	$\bar{x} \pm \sigma$	3.58 ± 6.72	6.40 ± 8.93	3.80 ± 7.00
	$\tilde{x}$	1.17	1.72	1.19
	IQR	12.18	8.69	2.33
ε_{e1} [mm]	$\bar{x} \pm \sigma$	1.69 ± 2.07	1.24 ± 1.01	1.65 ± 2.01
ε_{e2} [mm]	$\bar{x} \pm \sigma$	1.21 ± 1.34	1.29 ± 1.35	1.22 ± 1.34
ε_{e3} [mm]	$\bar{x} \pm \sigma$	1.26 ± 1.45	1.21 ± 1.18	1.25 ± 1.43

0.60 ± 0.35 mm) [26]. Even neglecting all further unquantified uncertainties, we have to deal with a propagated error ((catheter reconstruction = 0.6 mm)^2 + (registration = 1.77 mm)^2+(accuracy EMT = 0.7 mm)^2)^{½} of approximately 2 mm. This approximated error is in accordance to our measured median ε of 2.19 mm and proves an overall small deviation within the course of treatment. Further, considering the accumulation of the errors, it would be impossible to detect smaller shifts (<2 mm).

CT imaging and EMT measurements in free-breathing are altered by breathing motion. An attempt was made to eliminate the breathing motion by projecting the data with help of surface markers to exhale phase, see Kallis et al. [19] for details. With the proposed algorithm for motion compensation δ_F could be decreased 4.59 ± 8.54 mm, nonetheless error detection appears to be more reliable for measurements which are not distorted or corrupted by strong motion. Hence, breathing compensation seems satisfactory, but might also be focus of future research in order to ensure detection of shifts smaller than 2.00 mm or to use the measured data for EMT based automatic catheter reconstruction.

In order to eliminate the uncertainties connected to the different modalities, e.g. CT and EMT, Kellermeier et al. [18] suggested using the $EMT_{CT(1)}$, which mirrors the patient situation to the planning CT, as reference for all estimations of possible deviations. However, the comparison of the catheter traces both defined based on CT images proved deviations within a similar range than considering the EMT measurements. On average the differences was determined to 0.22 mm.

Beld et al. [27] used a MR-based system to track the source within phantoms with a accuracy of 0.4–0.6 mm. In contrast to an EMT based estimation (accuracy around 0.49 mm [17]), the motion of the catheters and the surrounding tissue can be proven and the localization of the source is not reconstructed but tracked in real-time.

In order to analyze possible occurring deviations the measured catheter traces were rigidly registered to the catheter traces defined in treatment planning and an overall TRE of 1.77 ± 0.66 mm was estimated. Nonetheless, one drawback of the study is that all presented results are influenced by the precision of the registration and, vice versa, occurring errors might influence the registration.

Götz et al. [28] compared different point set registration methods and found that the fast CPD algorithm (mean deviation = 2.55 mm) is non inferior to computational and time consuming algorithms like multi-dimensional scaling (mean deviation = 2.15 mm). Besides, with the lack of reliable ground truth, improved registration accuracy is not compulsory correlated to a more precise representation of the actual situation. Damato et al. [16] found even a mean residual registration error per catheter of 0.60 mm in a phantom study using straight catheters.

Moreover, online evaluation for quality assurance purposes prior to the irradiation is thinkable, even though iBT has a good clinical outcome [2] and low median deviations of 2.19 mm. Götz et al. [29] introduced a tool to automatically analyze the measured data for breast cancer patients. Such a tool, preferably directly connected to the measurement system, might be able to further improve the quality of the irradiation and decrease the occurrence of errors; especially shifts which might have a dosimetric influence. Particularly, in iBT boost therapy a high fraction dose (6 Gy) is applied in one fraction and even small shifts could influence the planned dose delivery.

Conclusion

To conduct an EMT measurement would yield valuable information whether the situation of treatment planning corresponds

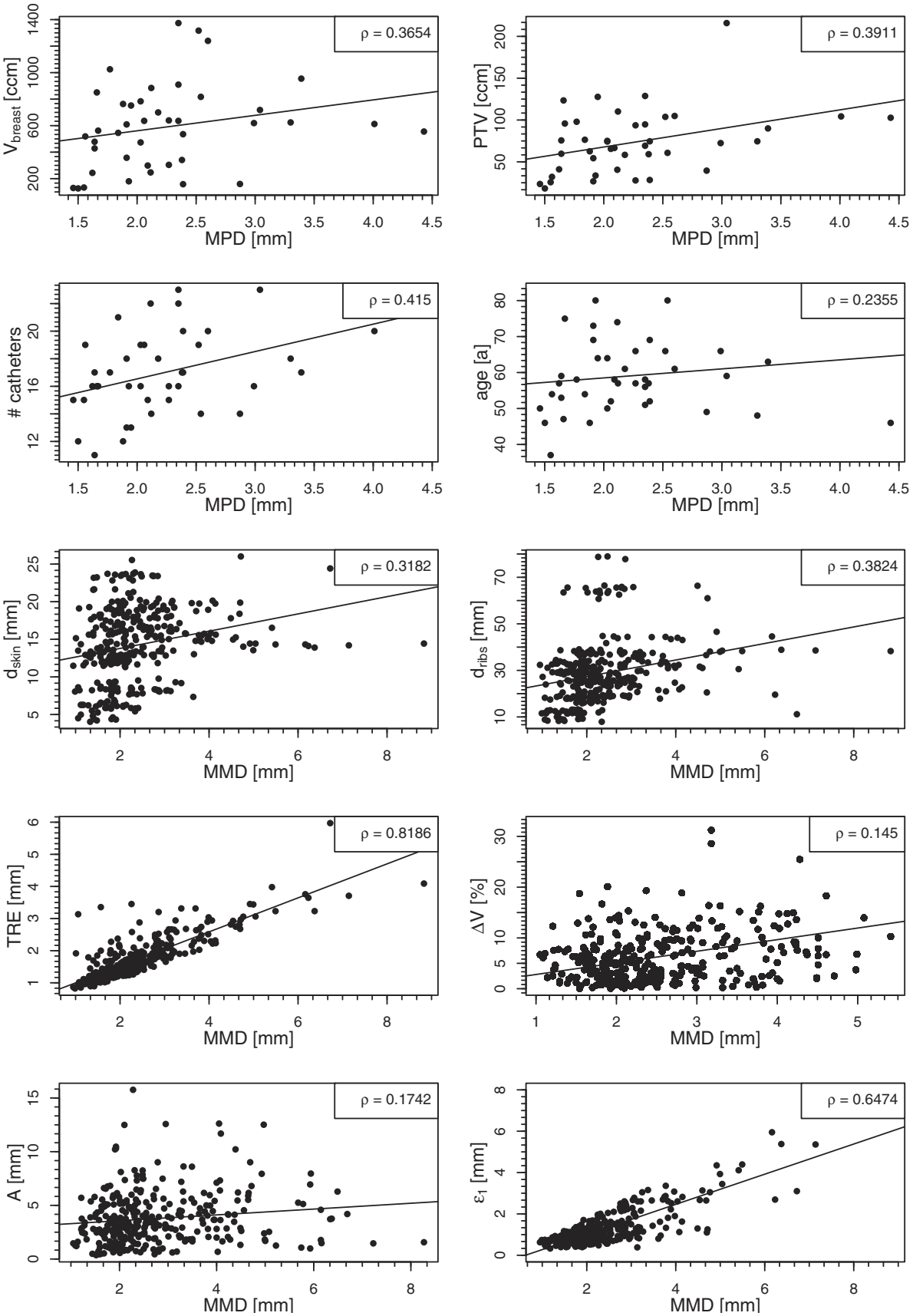

Figure 3. Summary of evaluated correlations.
Different features were compared to identify possible influences on the occurring deviations. The correlations were tested using the Spearman rank correlation with a confidence level of 0.95. PTV = planning target volume; DP = dwell positions; TRE = total registration error; MMD = median measurement deviation; MPD = median patient deviation; A = Amplitude; ε_1 = deviation in first principle component; ΔV = relative volume change; V_{breast} = breast volume; # catheter = number of catheters; d_{OAR} = distance to organ at risk (OAR).

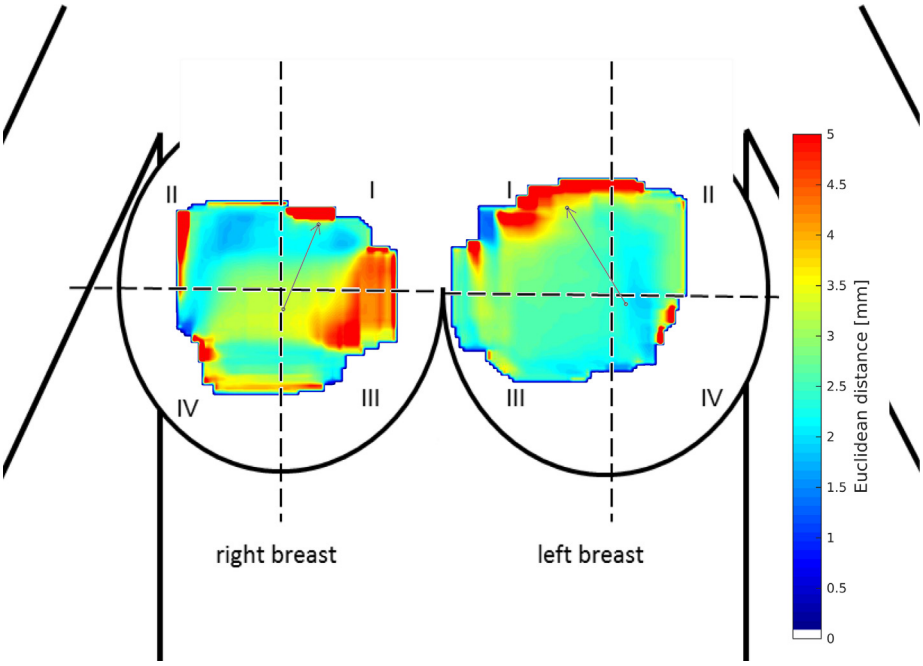

Figure 4. Partition of deviations in breast quadrants.
All dwell positions are centered on the mammilla, projected into the coronal plane and scaled according to third root of the breast volume relative to the smallest breast volume within the patient cohort in order to map all breast volumes to one central region. The figure shows the deviations for the right/left breast. The median errors of all DPs within arrays with a size of 2 mm*2 mm are summarized. The center presented by the cross marks the mammilla. The arrow presents the mean implantation direction over all patients. I. upper inner; II. upper outer; III. lower inner; IV. lower outer.

to the current situation. Detected errors, e.g. swaps and shifts could be directly corrected by shifting the catheters backwards or adapting the offset value of each catheter. Larger and inexplicable deviations however should result in acquiring a follow-up CT and adapting the treatment plan to the current situation.

Over all measurements, a median ε of 2.19 mm, a mean δ_F of 4.83 ± 3.95 mm and median ΔV of 5.28% was determined. Considering the used clinical safety margin around the tumor bed of 20.00 mm the occurring error seems marginal, however possibly critical for the surrounding OARs e.g. ribs and skin.

The presented results show that an EMT system, integrated into an afterloader has proven to be feasible and beneficial for quality assurance iBT. The error between the DPs could be reduced by adapting the treatment plan after the fourth fraction. No influence of the patients' age, breast volume, PTV, catheter length on the inter-fractional variations could be proven.

Declaration of Competing Interest

The authors declare that they have no known competing financial interests or personal relationships that could have appeared to influence the work reported in this paper. There is an unrestricted research framework with ELEKTA.

Acknowledgements

We would like to thank Marc Ziegler for various discussions and continuous support as well as Johanna Reichling, Moritz Schulz and Siti Masitho for assisting with the conducted measurements. The present work was performed in fulfillment of the requirements for obtaining the degree Dr. rer. biol. hum. of the Friedrich-Alexander-Universität Erlangen-Nürnberg (FAU).

Appendix A. Supplementary data

Supplementary data to this article can be found online at https://doi.org/10.1016/j.radonc.2019.08.012.

References

[1] Strnad V et al. 5-year results of accelerated partial breast irradiation using sole interstitial multicatheter brachytherapy versus whole-breast irradiation with boost after breast-conserving surgery for low-risk invasive and in-situ carcinoma of the female breast: a randomised, phase 3, non-inferiority trial. Lancet 2016;387:229–38.
[2] Strnad V et al. Accelerated partial breast irradiation: 5-year results of the German-Austrian multicenter phase II trial using interstitial multicatheter brachytherapy alone after breast-conserving surgery. Int J Radiat Oncol Biol Phys 2011;80:17–24.
[3] Njeh CF, Saunders MW, Langton CM. Accelerated Partial Breast Irradiation (APBI): a review of available techniques. Radiat Oncol 2010;5:1–28.
[4] Kindts I et al. Comparison of brachytherapy and external beam radiotherapy boost in breast-conserving therapy: patient-reported outcome measures and aesthetic outcome. Strahlenther Onkol 2019;195:21–31.
[5] Kindts I et al. A comparison of a brachytherapy and an external beam radiotherapy boost in breast-conserving therapy for breast cancer: local and any recurrences. Strahlenther Onkol 2019;195:310–7.
[6] Polgar C et al. Late side-effects and cosmetic results of accelerated partial breast irradiation with interstitial brachytherapy versus whole-breast irradiation after breast-conserving surgery for low-risk invasive and in-situ carcinoma of the female breast: 5-year results of a randomised, controlled, phase 3 trial. Lancet Oncol 2017;18:259–68.
[7] Schafer R et al. Quality-of-life results for accelerated partial breast irradiation with interstitial brachytherapy versus whole-breast irradiation in early breast cancer after breast-conserving surgery (GEC-ESTRO): 5-year results of a randomised, phase 3 trial. Lancet Oncol 2018;19:834–44.
[8] Tanderup K et al. Advancements in brachytherapy. Adv Drug Deliv Rev 2017;109:15–25.
[9] Kirisits C et al. Review of clinical brachytherapy uncertainties: analysis guidelines of GEC-ESTRO and the AAPM. Radiother Oncol 2014;110:199–212.
[10] Tanderup K et al. In vivo dosimetry in brachytherapy. Med Phys 2013;40:070902.
[11] Kertzscher G et al. In vivo dosimetry: trends and prospects for brachytherapy. Br J Radiol 2014;87:20140206.
[12] Johansen JG et al. Time-resolved in vivo dosimetry for source tracking in brachytherapy. Brachytherapy 2018;17:122–32.

[13] Smith RL et al. A method for verification of treatment delivery in HDR prostate brachytherapy using a flat panel detector for both imaging and source tracking. Med Phys 2016;43.
[14] Beaulieu L et al. Real-time electromagnetic tracking-based treatment platform for high-dose-rate prostate brachytherapy: clinical workflows and end-to-end validation. Brachytherapy 2018;17:103–10.
[15] Bert C, Kellermeier M, Tanderup K. Electromagnetic tracking for treatment verification in interstitial brachytherapy. J Contemp Brachytherapy 2016;8:448–53.
[16] Damato AL et al. A system to use electromagnetic tracking for the quality assurance of brachytherapy catheter digitization. Med Phys 2014;41:101702.
[17] Kellermeier M et al. Electromagnetic tracking (EMT) technology for improved treatment quality assurance in interstitial brachytherapy. J Appl Clin Med Phys 2017;18:211–22.
[18] Kellermeier M et al. Assessment of the implant geometry in fractionated interstitial HDR breast brachytherapy using an electromagnetic tracking system. Brachytherapy 2018;17:94–102.
[19] Kallis K et al. Introduction of a hybrid treatment delivery system used for quality assurance in multi-catheter interstitial brachytherapy. Phys Med Biol 2018;63:095008.
[20] Major T et al. Recommendations from GEC ESTRO Breast Cancer Working Group (II): target definition and target delineation for accelerated or boost partial breast irradiation using multicatheter interstitial brachytherapy after breast conserving open cavity surgery. Radiother Oncol 2016;118:199–204.
[21] Strnad V et al. Recommendations from GEC ESTRO Breast Cancer Working Group (I): target definition and target delineation for accelerated or boost partial breast irradiation using multicatheter interstitial brachytherapy after breast conserving closed cavity surgery. Radiother Oncol 2015;115:342–8.
[22] Strnad V et al. ESTRO-ACROP guideline: Interstitial multi-catheter breast brachytherapy as accelerated partial breast irradiation alone or as boost – GEC-ESTRO Breast Cancer Working Group practical recommendations. Radiother Oncol 2018;128:411–20.
[23] Alt H, Godau M. Computing the Frechet distance between 2 polygonal curves. Int J Comput Geometry Appl 1995;5:75–91.
[24] Zhen X et al. Comprehensive target geometric errors and margin assessment in stereotactic partial breast irradiation. Radiat Oncol 2017;12:151.
[25] Masitho S et al. OC-0075 Error detection using an electromagnetic tracking system in multicatheter interstitial brachytherapy. Radiother Oncol 2019;133:S35.
[26] Kallis K et al. Impact of inter- and intra-observer variabilities of catheter reconstruction on multi-catheter interstitial brachytherapy of breast cancer patients. Radiother Oncol 2019;135:25–32.
[27] Beld E et al. MR-based source localization for MR-guided HDR brachytherapy. Phys Med Biol 2018;63:085002.
[28] Goetz TI et al. Technical Note: a comparison of point set registration methods for electromagnetic tracking. Med Phys 2019.
[29] Goetz TI et al. A tool to automatically analyze electromagnetic tracking data from high dose rate brachytherapy of breast cancer patients. PLoS ONE 2017;12.